NATIONAL SCIENCE FOUNDATION
Washington, D.C. 20550

FINAL PROJECT REPORT
NSF FORM 98A

PLEASE READ INSTRUCTIONS ON REVERSE BEFORE COMPLETING

PART I-PROJECT IDENTIFICATION INFORMATION

1. Institution and Address	2. NSF Program	3. NSF Award Number
Georgia Institute of Technology Atlanta, GA 30332	Separations Processes	ENG 7926304
	4. Award Period From 7/1/80 To 7/1/82	5. Cumulative Award Amount $65,000

6. Project Title
The Effect of Impurities on Occlusion Formation During Crystallization from Solution

PART II-SUMMARY OF COMPLETED PROJECT *(FOR PUBLIC USE)*

The critical crystal size required for the formation of solvent inclusions during the crystallization of potassium aluminum sulfate dodecahydrate was found to be significantly altered in the presence of small concentrations of the ionic impurities nickel and copper. The critical crystal size increased with increasing nickel ion concentration and decreased with increasing copper ion concentration. The concentration of copper in grown crystals was approximately an order of magnitude greater than the concentration in crystals grown at similar conditions.

The formation of solvent inclusions in terephthalic acid crystals in the presence and absence of impurities was also examined. Inclusions of up to 3% of the total crystal volume were observed in TPA crystals of 0.1-0.5 cm. These inclusions were formed upon recrystallization or upon aging.

A computer simulation of crystal growth was modified and used to predict the effect of adsorbed impurities on the critical size for inclusion formation by assuming the blocking of active sites for growth during the crystallizaiton process.

Publication Citations

1. AIChE Symposium Series #212 Vol. 78, page 37 (1982)

2. AIChE Journal (In Review)

PART III-TECHNICAL INFORMATION *(FOR PROGRAM MANAGEMENT USES)*

1. ITEM *(Check appropriate blocks)*	NONE	ATTACHED	PREVIOUSLY FURNISHED	TO BE FURNISHED SEPARATELY TO PROGRAM	
				Check (✓)	Approx. Date
a. Abstracts of Theses		X			
b. Publication Citations		X			
c. Data on Scientific Collaborators	X				
d. Information on Inventions	X				
e. Technical Description of Project and Results		X			
f. Other *(specify)*					

2. Principal Investigator/Project Director Name *(Typed)*	3. Principal Investigator/Project Director Signature	4. Date

NSF Form 98A (5-78) Supersedes All Previous Editions

Form Approved OMB No. 99R0013

EFFECT OF IMPURITIES ON OCCLUSION FORMATION DURING CRYSTALLIZATION FROM SOLUTION

Final Technical Report
NSF Grant # ENG 7926304

Allan S. Myerson
School of Chemical Engineering
Georgia Institute of Technology
Atlatna, GA 30332

PART 1: POTASSIUM ALUMINUM SULFATE

Introduction

The presence of pockets of solvent trapped as a second phase (occlusions) in crystals grown from solution and from the melt has been widely reported on the literature (1-10). Previous work (1-5) has indicated that occlusion formation will increase with increasing crystal growth rate and will decrease with increasing interfacial temperature gradient. Theoretical studies of occlusion formation employing the constitutional supercooling criterion (11,12), and those employing perturbation theory (13,15), indicate that the interface can only be stable (hence no occlusion formation) in the presence of a finite interfacial temperature gradient. Brice and Bruton (16) postulated that interfacial kinetics could produce a stabilizing effect on the interface which would decrease with increasing crystal growth rate. Slaminko and Myerson (17) experimentally studied the growth of single crystals of sodium chloride and potassium aluminum sulfate dodecahydrate. They reported a critical crystal size (at a given set of conditions) below which occlusions did not form.

The existence of this critical crystal size below which occlusions do not occur suggests the possibility of controlling occlusion formation in industrial crystallizers through control of the crystal size distribution. Industrial crystallizers, however, often contain low concentrations of a variety of impurities. The effect of various commonly occurring impurities on the critical crystal size for occlusion formation must, therefore, be examined.

Background

It is well known that low concentrations of impurities can dramatically effect the growth rates and habits of crystals grown from solution. Many investigators (18,19) have examined this phenomena, however, there is yet

no generally accepted theory to explain the mechanisms by which impurities participate in the crystallization process. There are several ways an impurity may effect crystal growth rate and habit. These include:

1. Changing of the solution properties.
2. Changing the properties of the solid-liquid interface.
3. Selective adsorption of the impurity on the various crystal faces thus disrupting the growth of those faces and changing the surface energies.

It is not possible to predict, however, how a given impurity will act in a given system.

Several investigators (19-20) have studied the effects of impurities on the formation of dendrites. Buckley (18) reported that low concentrations of certain dyes ($5x10^{-5}$) gram/gram solute) caused $KClO_3$ to grow dendritically. Saratorkin (20) found that 0.001 percent pectic acid inhibited the formation of dendrites of NH_4Cl grown from aqueous solution. He also indicated that various impurities could alter the shape, direction, and degree of branching of NH_4Cl dendrites. In order for an occlusion to form, the crystal liquid interface must break up and grow in an unstable manner. The results reported in the literature indicate that some impurities can cause dendritic (hence unstable) growth while others can inhibit unstable growth. It therefore, seems likely that various impurities should effect both the degree of occlusion formation and the critical size for occlusion formation. The purpose of this paper is the experimental verification of the above hypothesis through an examination of the effect of nickel and copper ions on the occlusion formation, and critical size for occlusion formation during the growth of single crystals of potassium aluminum dodecahydrate from aqueous solution.

Experimental

In order to experimentally measure solvent occlusion as a function of crystal size during the crystallization of solutes from aqueous solution, a flow crystallizer similar to one used by Slaminko and Myerson (17) was employed. A schematic of the apparatus is shown in Figure 1. Solution at a controlled flow rate and supersaturation flows over a crystal suspended on the needle tip. Heat and mass transfer are well-defined in this geometry. The fluid velocity can be raised to a value where it does not affect growth rates indicating little mass transfer influence. The change in supersaturation in the solution during each experiment was small (2% or less) and should have had a negligible effect. The average growth rate was obtained from the weight gain of the crystal. The amount of solvent entrapped was obtained by analysis of the crystals employing atomic absorption spectrometry. In those systems that form hydrates, only water exceeding the stoichiometric amount within the solid was taken as impurity. The accuracy of the excess water determination was no worse than ± 3% by weight. This apparatus was used to grow $KAl(SO_4)_2 \cdot 12H_2O$ from aqueous solution with and without impurities present. Solubility data for $KAl(SO_4)_2 \cdot 12H_2O$ in water were obtained from Seidell and Linke (21).

Experiments were conducted at undercoolings of 1 and 2°C, nickel ion concentrations of 100, 200 and 500 ppm and copper ion concentrations of 100 and 200 ppm. Nickel was added to the solution as nickel chloride and copper was added as copper chloride. Experiments were conducted at a variety of growth times so as to obtain a variety of crystal sizes at each undercooling. The crystallization temperature was 29°C for all experiments. A flow rate of 0.4 m/sec was used to minimize mass transfer effects. Crystals were initially about 5×10^{-4} m equivalent spherical diameter based on their mass.

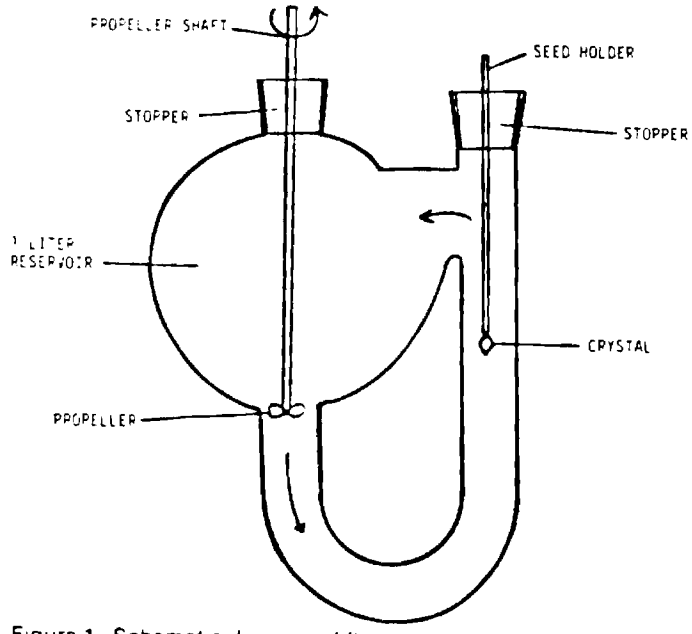

Figure 1 Schematic diagram of flow crystallizer

Results and Discussion--Potassium Aluminum Sulfate

Results for the growth of potassium aluminum sulfate dodecahydrate from pure aqueous solution are presented in Table 1.

TABLE 1

Dependence of Occlusion Formation on Crystal Size in the Absence of Impurities.

Applied Undercooling (°C)	Growth Velocity m/sec x 10^8	Final Diameter m x 10^3	Mass Percent Occluded H_2O
1	2.5	1.5	0
1	2.2	2.0	0
1	1.9	2.3	0
1	1.9	2.6	0
1	1.8	2.7	4.3
1	2.0	3.0	9.2
1	2.1	3.3	11.0
1	2.2	3.8	16.6
2	5.0	2.4	0
2	4.1	2.6	0
2	4.2	2.8	0
2	3.0	3.2	10
2	3.6	3.5	13
2	4.0	2.7	18

These results indicate a critical crystal size of $2.8X10^{-3}$m at an average growth velocity of $4.0X10^{-8}$ m/s (2°C undercooling) and $2.6X10^{-3}$ at an average growth velocity of $2.1X10^{-8}$ m/s (1°C undercooling). These results closely reproduce those reported by Slaminko and Myerson (17). Results are presented in Tables 2 and 3 showing the effect of nickel ion on the growth velocity and critical size. The addition of nickel to the solution had little effect on the growth velocity. The average crystal growth velocities at 2°C undercooling were $4.0X10^{-8}$, $4.0X10^{-8}$, $3.9X10^{-8}$ and $3.8X10^{-8}$ m/s at nickel ion concentrations of 0, 100, 200 and 500 ppm, respectively. The addition of nickel, however, increased the critical crystal size for occlusion formation. The critical size increased with increasing nickel concentration (at 2° undercooling) from $2.8X10^{-3}$ m to $4.3X10^{-3}$ m as the nickel concentration increased from 0 to 500 ppm.

TABLE 2

Dependence of Occlusion Formation on Crystal Size and Nickel Ion Concentration During the Growth of Single Crystals of Potassium Aluminum Sulfate Dodecahydrate.

Nickel Ion Concentration (ppm)	Growth Velocity m/sec x 10^8	Final Diameter m x 10^3	Mass Percent Occluded H_2O
100	3.9	1.5	0
100	3.6	2.1	0
100	4.0	2.7	0
100	4.1	2.9	0
100	4.0	3.0	0
100	3.5	3.4	2.8
100	3.6	3.8	7.1
100	4.2	4.0	9.5
100	4.7	4.2	10.0
200	3.6	2.6	0
200	3.8	2.9	0
200	4.0	3.2	0
200	4.2	3.2	0
200	3.5	3.5	0
200	4.1	3.7	4.0
200	4.4	4.1	4.0
200	4.5	4.3	5.0
200	3.8	4.4	7.0
200	3.7	4.6	6.0
200	3.4	4.8	10.0
200	3.5	5.0	15.0
500	3.2	2.8	0
500	4.0	3.0	0
500	4.0	3.1	0
500	3.8	3.5	0
500	4.0	3.8	0
500	3.3	4.0	0
500	4.5	4.3	5.0
500	3.7	4.4	8.0
500	3.6	4.5	4.0
500	3.8	4.7	8.0
500	3.9	4.9	11.0
500	3.2	5.2	13.0

Applied Undercooling = 2°C

TABLE 3

Dependence of Occlusion Formation on Crystal Size and Nickel Ion Concentration During the Growth of Single Crystals of Potassium Aluminum Sulfate Dodecahydrate.

Nickel Ion Concentration (ppm)	Growth Velocity m/sec x 10^8	Final Diameter m x 10^3	Mass Percent Occluded H_2O
100	1.9	1.2	0
100	2.1	1.9	0
100	2.0	2.2	0
100	1.8	2.5	0
100	1.7	2.7	0
100	2.0	3.0	2.1
100	1.9	3.3	9.0
100	1.8	3.7	15.0
100	1.6	4.0	19.0

Undercooling = 1°C

The concentration of nickel present in crystals grown at 1 and 2°C of undercooling at nickel concentrations in solution of 100 ppm are shown in Table 4. The concentrations reported in Table 4 are those of the nickel in the crystalline portion of the crystal and do not include the nickel associated with the occluded solution. Results indicate a small, but finite average nickel concentration of 0.13 and 0.12 ppm at 1 and 2°C of undercooling respectively.

TABLE 4

Concentration of Nickel in Crystals Grown in the Presence of 100 ppm Nickel.

Undercooling (°C)	Ni Concentration (ppm)
1	0.12
1	0.10
1	0.10
1	0.15
1	0.16
1	0.17
1	0.18
1	0.11
1	0.09
2	0.13
2	0.09
2	0.10
2	0.14
2	0.15
2	0.12
2	0.14
2	0.11
2	0.14

Results are presented in Tables 5 and 6 showing the effect of copper ion on the growth velocity and critical size. The addition of copper ion had little effect on the growth velocity. The average growth velocities at 1°C undercooling were $2.0X10^{-8}$, $2.1X10^{-8}$ and $2.2X10^{-8}$ m/s at copper ion concentrations of 0, 100 and 200 ppm, respectively. Copper, however, decreased the critical

crystal size for occlusion formation. The critical size decreased with increasing copper concentration (at 1°C undercooling) from $2.6X10^{-3}$ m to $1.7X10^{-3}$ m as the copper was concentration increased from 0. to 200 ppm.

TABLE 5

Dependence of Occlusion Formation on Crystal Size and Copper Ion Concentration During the Growth of Single Crystals of Potassium Aluminum Sulfate Dodecahydrate.

Copper Ion Concentration (ppm)	Growth Velocity m/sec x 10^8	Final Diameter m x 10^3	Mass Percent Occluded H_2O
100	2.0	1.1	0
100	2.1	1.9	0
100	1.9	2.0	0
100	2.3	2.2	0
100	2.5	2.4	1.6
100	1.8	2.8	7.3
100	2.0	3.1	10.1
100	2.2	3.4	13.4
200	2.1	1.0	0
200	2.2	1.3	0
200	1.8	1.5	0
200	2.0	1.6	0
200	2.2	1.7	0
200	2.3	2.0	1.5
200	2.3	2.5	6.3
200	2.4	3.1	9.8
200	2.5	3.7	14.3

Undercooling = 1°C Temperature = 29°C

TABLE 6

Dependence of Occlusion Formation on Crystal Size and Copper Ion Concentration During the Growth of Single Crystals of Potassium Aluminum Sulfate Dodecahydrate.

Copper Ion Concentration (ppm)	Growth Velocity m/sec x 10^8	Final Diameter m x 10^3	Mass Percent Occluded H_2O
100	4.4	1.0	0
100	3.7	1.3	0
100	4.0	1.8	0
100	5.5	1.9	0
100	6.7	2.2	3.2
100	4.9	2.9	11.4
100	5.1	3.3	16.2
100	5.0	3.7	15.5
200	5.1	1.0	0
200	4.1	1.2	0
200	3.6	1.4	0
200	5.2	1.5	0
200	5.4	1.8	2.0
200	4.9	2.5	7.2
200	5.0	2.9	10.4
200	4.8	3.5	15.5

Undercooling = 2°C Temperature = 28°C

The concentration of copper present in crystals grown at 1 and 2°C of undercooling at copper concentration in solution of 100 ppm are shown in Table 7. The average copper concentrations were 1.4 and 1.5 ppm at 1 and 2°C and undercooling, respectively.

TABLE 7

Undercooling (°C)	Cu Concentration (ppm)
1	0.84
1	0.93
1	1.0
1	1.5
1	1.7
1	1.6
1	1.5
1	2.3
2	1.1
2	1.2
2	1.6
2	1.5
2	1.4
2	1.8
2	1.3
2	2.1

Previous work (1) has indicated that the amount of solvent trapping in $KAl(SO_4)_2 \cdot 12H_2O$ crystals larger than $3.6X10^{-3}$ m (grown without impurities present) are not a function of size. If the amount of trapped solvent is constant with size in large crystals (crystals considerably larger than the critical size) it indicates that a constant percentage of new crystalline material added during the growth process is trapped solvent. The overall degree of solvent trapping in a crystal growing from its critical size should start at zero, increase with increasing crystal size and asymptotically approach a maximum value. This phenomena was experimentally observed by Slaminko and Myerson (17). The presence of nickel, however, both increases the critical size and at sizes larger than the critical size decreases the degree of solvent trapping. These results indicate that nickel ion is able to stabilize their interface in some way. The low concentration of nickel adsorbed on the crystal surface along with the fact that nickel concentration had little effect on the crystal growth velocity both indicate that the mechanism by which nickel affects the crystal growth process must involve changes in the solution and/or interfacial properties of the systems.

The results employing copper ion as an impurity were exactly opposite to those of nickel ion. The copper ion both decreased the critical size for formation and at sizes greater than the critical size increased the degree of solvent trapping. The concentration of copper adsorbed on the crystal surface was an order of magnitude greater than in the experiments employing nickel ion. The results indicate that the adsorption of copper on the surface tends to destabilize the interface, hence promoting solvent trapping.

The results presented in this paper indicate that low concentrations of ionic impurities can both stabilize and destabilize the crystal interface. The latter case, which involves adsorption on the crystal surface thereby

preventing lateral spread of a new growth layer, is consistent with theories the effect of impurities on crystal growth (22). The mechanism by which nickel ion stabilizes the crystal interface without significant adsorption on the surface, however, is unclear and will require additional study.

References

1. Myerson, A. S., "Impurity Capture and Crystal Growth," Ph.D. Dissertation, University of Virginia, January 1977.
2. Myerson, A. S. and D. J. Kirwan, Ind. Eng. Chem. Fundam., 16, 414 (1977).
3. Myerson, A. S. and D. J. Kirwan, Ind. Eng. Chem. Fundam., 16, 420 (1977).
4. Myerson, A. S., R. A. Nidel and D. J. Kirwan, 70th Annual Meeting of the AIChE, New York, New York, November 1977.
5. Edie, D. D. and D. J. Kirwan, Ind. Eng. Chem. Fundam., 12, 100 (1973).
6. Wilcox, W. R., J. Appl. Phys., 35, 636 (1963).
7. Cheng, C. S., D. A. Irvin and B. G. Kyle, AIChE Journal, 13, 1331 (1970).
8. Denbigh, K. G. and E. T. White, Chem. Eng. Sci., 21 739 (1966).
9. Ozum, B. and D. J. Kirwan, AIChE Symp. Ser., No. 153, 72 (1976).
10. Terwilliger, J. P. and S. F. Dizio, Chem. Eng. Sci., 21 1331 (1970).
11. Tiller, W. A., K. A. Jackson, J. W. Rutter and B. Chalmers, Acta Met., 1, 428 (1953).
12. Tiller, W. A., J. Crystal Growth, 2, 69 (1968).
13. Mullins, W. W. and R. F. Sekerka, J. Appl. Phys., 35, 444 (1964).
14. Mullins, W. W. and R. F. Sekerka, J. Appl. Phys., 34, 323 (1963).
15. Sekerka, R. F., J. Crystal Growth, 3, 71 (1968).
16. Brice, J. C. and T. M. Bruton, J. Crystal Growth, 26, 59 (1974).
17. Slaminko, P. and A. S. Myerson, AIChE Journal, 27, 1029 (1981).
18. Mullin, J. W., "Crystallization," CRC Press, Cleveland (1971).
19. Buckley, H. E., "Crystal Growth," Wiley, New York (1951).
20. Saratorkin, A. D., "Dendritic Crystallization," Consultants Bureau (1959).

21. Siedell, A. and W. F. Linke, "Solubilities of Inorganic and Metal Organic Compounds," Vol. I and II, American Chemical Society, Washington, D.C. (1958).

22. O'Hara, M. and R. C. Reid, "Modeling Crystal Growth Rates from Solution," Prentice Hall, Englewood, New Jersey (1978).

PART 2--Inclusion in Terephthatic Acid

INTRODUCTION

In recent years improved processes for the manufacture of terephthalic acid (TPA) have led to the development of processes for the direct esterification of TPA with ethylene glycol. This route to the formation of polyethylene terephthalate (PET) has significant economic advantages (Hizikata (1977)) when compared with the route employing dimethyl terephthalate (DMT). A requirement of the direct esterification route is a pure grade of TPA virtually free of impurities which cause unwanted coloring of the product PET. The impurities in TPA manufactured by the oxidation of paraxylene are typically intermediate and by-products of the oxidation such as 4-carboxybenzaldehyde (4-CBA), o- and m-phtalic acids, p-toluic acid and p-acetylbenzoic acid. 4-CBA is probably the most difficult of these impurities to remove and its concentration in TPA serves as a practical criterion of TPA purity.

Purification of TPA has been the subject of intensive research of the years and a multitude of techniques have been proposed. A summary of these techniques appears as Table I. A large number of the TPA purification techniques employ crystallization (from the vapor or from the liquid) as a purification step (Maclean (1960), Kurtz (1965), Olsen (1970)). It has been reported (Fujita et al. (1968)) that recrystallization alone does not normally reduce 4-CBA concentrations in TPA crystals to the desired level. In a recent paper Myerson and Gaines (1982) reported that TPA crystals underwent an irreversible change of habit (known as crystal aging) when immersed in their own saturated solution. The rate of this change of shape was reported to be a strong function of temperature and resulted in an increase in crystal purity. It is the purpose of this study to present several observations which may explain the limitations of crystallization or aging as a purification method.

TPA Recrystallization and Aging

Recrystallization and aging experiments were conducted in a batch suspension crystallizer shown in Figure 1. It consists of a glass-lined stainless steel tube with flat glass windows at each end and held in place by a cover plate and bolts. The chamber is equipped with a magnetic stirrer. Temperature is controlled in the crystallizer by immersion in a constant temperature bath or through controlled resistance heating. Observation and photography of the growing or aging crystals was possible through the use of a stereozoom microscope.

Pure and fiber grade TPA supplied by the Amoco Oil Company was slowly recrystallized in the batch suspension from aqueous solutions at temperatures ranging from 150-200°C. The resulting crystals were rod shaped, bound mostly by three or four planes parallel to the long dimension of the crystals. Frequent twinning was observed along the long axis parallel to the crystallographic c-axis. The crystals ranged in size from 0.1-0.5 cm (measured along the long axis) with the average being 0.2 cm.

Aging experiments were carried out in the same apparatus holding the temperature constant. Aging experiments showed a gradual transformation of the initial globular crystals to needles indistinguishable from those obtained from crystallization experiments. The transformation of the particles took approximately 15 hours at 200°C. These results are similar to those reported by Myerson and Gaines (1982) in their study of TPA aging.

The crystal structure of two polymorphic forms of TPA was described by Bailey and Brown (1967). The crystal structures of the crystals obtained experimentally in this work were investigated employing x-ray diffraction of both polycrystalline and single crystal samples. Results of the x-ray

analysis were consistent with polymorphic form I as reported by Bailey and Brown. The unit cell parameters determined along with those reported by Bailey and Brown appear in Table II. No form II was detected in polycrystalline specimens. The crystals were also examined employing scanning electron microscopy (SEM). SEM photographs of the crystals viewed along their long dimension revealed the frequent occurrence of large longitudinal cavities often positioned close and parallel to the twinning plane. Two such crystals appear in Figures 2 and 3.

Quantitative determination of the volume of the inclusions observed in the SEM photography was accomplished through density measurement. The theoretical density of TPA (polymorphic form I) was calculated from the unit cell parameters given in Table II and yielded a value of 1.573 g/cm^3. The volume of the inclusions filled with solution will result in a decrease in the density of the crystal porportional to the included volume. At 25°C the density of TPA as a function of the volume of included solution can be expressed by the relation:

$$\rho = (1.573 - 5.73 \times 10^{-3} I) \qquad [1]$$

where ρ is the density in g/cm^3 and I is the included volume percent in the crystal.

The density of the grown and aged TPA crystal was measured employing 2 ml pycnometers at 25°C with water as the liquid media. Considering the low TPA solubility in water at room temperature (app. 10 ppm, Stautzenberger and Maclean (1971)) no correction on solubility was applied. The average density obtained for aged and crystallized TPA was 1.566 ± 0.006 g/cm^3 which results in an average calculated value of the included volume of 1.2%.

The presence of solvent inclusions in TPA prepared by crystallization and by crystal aging limits the degree of purification that can be obtained by

these processes. The final concentration of an impurity in TPA purified by the processes will, therefore, depend on the concentration of the impurity in the included solution and the size of the inclusion. In previous studies of solvent inclusions (Myerson and Kirwan (1977), Slaminko and Myerson (1981), Senol and Myerson (1982)) it has been demonstrated that the degree of solvent inclusion increases with increasing crystal growth rate and is a function of crystal size and the impurities present in solution. The effect of these variables on the formation of solvent inclusions in TPA, however, will require a carefully controlled experimental study. The results of this work indicate, however, that under both slow (aging) and rapid (recrystallization) growth conditions the degree of inclusion in TPA crystals is identical so that extremely slow growth conditions might be required for the preparation of inclusion-free TPA.

List of Tables

TABLE I PROPOSED METHODS OF TPA PURIFICATION

PHASE	METHOD		COMMENTS
Vapor Phase	Sublimation	Maclean (1960)	Fluidized Bed
	Sublimation, oxidation/hydrogenation	Bryant et al. (1970)	Metal Catalyst
Liquid Phase	Oxidation	Tate (1962) Wise and Meyer (1963)	Activated Carbon Treatment
		Shigeyasu et al. (1968)	Ion Exchange Treatment
		Taylor et al. (1971)	In Acetic Anhydride Solution
		Stautzenberger and Maclean (1971)	Weak Acid Solution
		Ichikawa and Suzuki (1969)	Aqueous Pyridine Solution
	Other	Ringwald (1963)	Sulfuric Acid Treatment
		Kurtz (1965)	Recrystallization
		Swakon (1963)	CO treatment, activated carbon
		Olsen (1970)	Controlled Continuous Crystallization
		Hensley and Towle (1967)	Activated Carbon
		Witt and Blay (1972)	Iodine or Bromine Catalyst
		Blay (1973)	Mixtures of Acids and Catalysts

TABLE II UNIT CELL PARAMETERS OF TPA FORM I

	Measured	Bailey and Brown (1967)
a_o	7.736 Angstroms	7.730 Angstroms
b_o	6.444 Angstroms	6.443 Angstroms
c_o	3.7504 Angstroms	3.749 Angstroms
α	91.51°	92.75°
β	109.12°	109.15°
γ	95.77°	95.95°

List of Figures

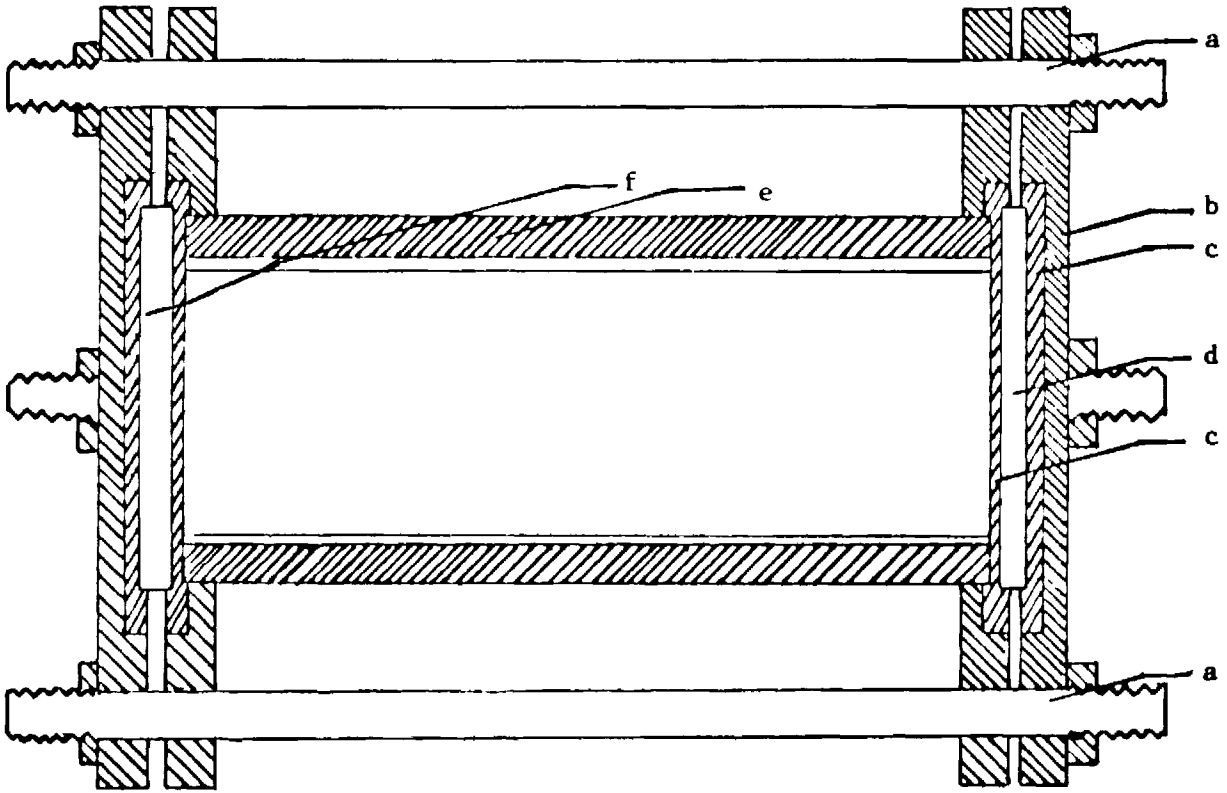

Figure 1: Aging Cell. (a)1/4" connecting rod; (b) 4" diameter by 1/4" thick steel frame plate; (c) teflon gasket; (d) 2" diameter by 1/4" thick tempered sight glass; (e) 1 1/2" nominal diameter schedule 80 stainless steel pipe; (f) 1 1/2" OD tempered sight glass.

REFERENCES

Bailey, M., and C. J. Brown, "The Crystal Structure of Terephtalic Acid," Acta Crystal. 22, 387 (1967).

Blay, J. A., "Thermal Purification of Terephtalic Acid Using a Carboxylic Acid-C_8 Aromatic Solvent," U. S. Patent 3,717,674 (Filed Nov. 29, 1968; issued Feb. 20, 1973).

Bryant, H. S., et al., "Terephtalic Acid Purification Process," U. S. Patent 3,522,298 (filed Dec. 13, 1966; issued July 28, 1970).

Fujita, Y., et al., "Behavior of 4-Formylbenzoic Acid in Terephtalic Acid Synthesis," Symposium on Foreign Developments in Petrochemicals, American Chemical Society, Atlantic City, Sept. 8, 1968.

Hensley, A. L., and P. H. Towle, "Purification of Water-Insoluble Aromatic Dicarboxylic Acids Obtained by Catalytic Liquid Phase Oxidation with Molecular Oxygen," U. S. Patent 3,344,177 (Filed Feb. 21, 1964; issued Sept. 26, 1967).

Hizikata, M., "New Process for Fiber-grade High-purity Terephtalic Acid (HTA)," Chem. Econ. Eng. Review, 9, 32 (1977).

Ichikawa, Y., and N. Suzuki, "Process for preparation of High Purity Terephtalic Acid," U. S. Patent 3,431,296 (Filed Sept. 21, 1964; issued Mar. 4, 1969).

Kurtz, K. K., "Acid Purification Process," U. S. Patent 3,171,856 (Filed Jan. 4, 1962; issued Mar. 2, 1965).

Maclean, D., "Purification of Carboxylic Acids," U. S. Patent 2,923,736 (Filed Nov. 18, 1957; issued Feb. 2, 1960).

Myerson, A. S. and D. J. Kirwan, "Impurity Trapping During Dendritic Crystal Growth," Ind. Eng. Chem., Fundam., 16, 414 (1977).

Myerson A. S., and S. Gaines, "Removal of Impurities Through Crystal Aging," AIChE Symposium Series (1982) in press.

Myerson, A. S., and D. J. Kirwan, "Impurity Trapping During Dendritic Crystal Growth," Ind. Eng. Chem. Fund., 16, 420 (1977).

Olsen, G. P., "Continuous Crystallization in a Plurality of Cooling Stages Using Dilutions by Cooled Solvent of Feed to Each Stage," U. S. Patent 3,497,552 (Filed July 18, 1966; issued Feb. 24, 1970).

Ringwald, E. L., "Purification of Terephtalic Acid," U. S. Patent 3,080,421 (Filed Nov. 18, 1958; issued Mar. 5, 1963).

Senol, D. E., and A. S. Myerson, "Effect of Impurities on Occlusion Formation During Crystallization From Solution," AIChE Symposium Series (1982) in press.

Shigeyasu, M., et al., "Purification of Terephtalic Acid," U. S. Patent 3,410,897 (Filed Oct 12, 1964; issued Nov. 12, 1968).

Slaminko, P., and A. S. Myerson, "The Effect of Crystal Size on Occlusion Formation During Crystallization From Solution," AIChE Journal 27, 1029 (1981).

Stautzenberger, A. L., and A. F. Maclean, "Purification of Organic Acids," U. S. Patent 3,629,328 (Filed May 20, 1969; issued Dec. 21, 1971).

Swakon, E. A., "Aromatic Acid Purification," U. S. Patent 3,115,521 (Filed Apr. 29, 1960; issued Dec. 24, 1963).

Tate, C. W., "Purification of Phtalic Acids," U. S. Patent 3,047,621 (Filed Apr. 6, 1959; issued July 31, 1962).

Taylor, W. E., et al., "Purification of Terephtalic Acid," U. S. Patent 3,574,727 (Filed Oct. 16, 1967; issued Apr. 13, 1971).

Wise, R. H., and D. H. Meyer,"Purification of Terephtalic Acid," U. S. Patent 3,102,137 (Filed June 1, 1959; issued Aug. 27, 1963).

Witt, E. R., and J. A. Blay, "Purification of Terephtalic Acid," U. S. Patent 3,654, 350 (Filed Jan. 14, 1970; issued Apr. 4, 1972).

COMPUTER SIMULATION

The crystallization process is one of great complexity. A mathematical model of the problem is essentially that of a moving boundary problem involving an interfacial rate process and simultaneous heat and mass transfer in the liquid phase. Factors such as dendritic crystal growth and interfacial crystallization kinetics complicate the process a great deal. Experimentally it is difficult to devise and perform experiments which will measure and control the desired variables, and allow their variation over a large range of conditions. In a situation of this type where both analytic and experimental methods fail to supply the needed information, a computer simulation can be of use.

A. Description of Simulation

Crystallization is a moving boundary problem with simultaneous heat and mass transfer. Numerical solutions of this type of problem are similar to those found in the literature (1). The simulation considers variations with time and two spatial coordinates parallel and perpendicular to the primary growth direction. A flow chart of the program is given in Figure 7. Crystal growth occurs first, followed by heat transfer, mass transfer and melting (dissolution) for the same time interval.

The program consists of four subroutines and the main program. The subroutines are growth (Grow), heat transfer (Heat), mass transfer (Mass), and melting (Melt). A listing of program appears in Appendix (A).

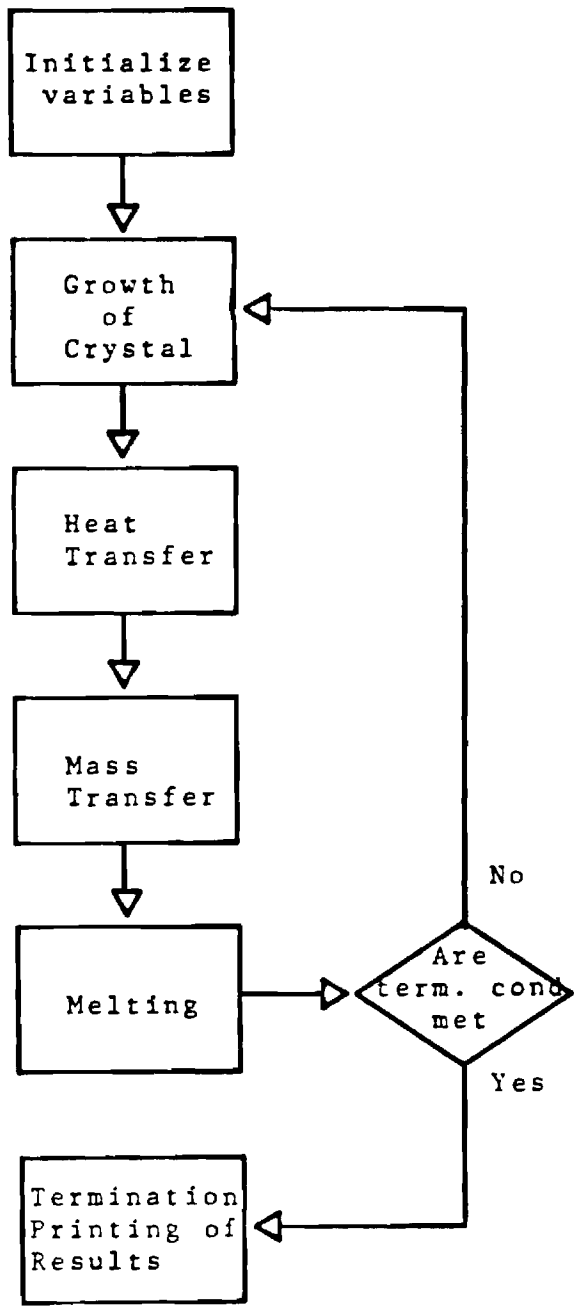

Figure 7. Flowchart of Simulation.

The first part of the program initializes the crystal growth process. The crystallization process is carried out in a 100 X 100 matrix. At each point in the matrix a value is stored relating to the state of that site at a particular time. A 2 means it is all crystal and a number between zero and one represents liquid at the indicated mole fraction. To begin the crystallization process one or more sites are chosen at random in the middle of the matrix at the bottom so that growth occurs in the positive direction. Heat is released and the second component is rejected when crystallization occurs. The heat of crystallization is evenly distributed to its nearest neighbors. The rejected second component is also evenly distributed among the nearest liquid neighbors and results in a drop in concentration of the crystallizing component at these sites; hence, a drop in the equilibrium freezing temperature at these sites. With this step, control is shifted to the growth routine.

The growth routine allows crystal growth for a finite time interval only at those sites adjacent to existing crystal. The equilibrium freezing temperature is then calculated from the following relationship:

$$T_f = \frac{H}{[1- AS \ln (1-C)]} \tag{45}$$

where T_f = equilibrium freezing temperature

AS = constant (varies with substance being modeled)

H = pure component freezing temperature

C = mole fraction of crystallizing component

A critical growth velocity is then calculated for each possible growth site from:

$$V = a\,(T_f - T)^n \tag{46}$$

where V = crystal growth velocity

a = constant

T = actual temperature

T_f = equilibrium freezing temperature

n = constant

The constants a and n are obtained from experimental crystal growth data found in the literature.

Sites which are not adjacent to existing crystal are given velocities of zero. All crystal growth velocities are then normalized by the maximum velocity calculated, resulting in values between zero and one. The normalized velocities are then used as the probability of a site growing one unit in 1/(maximum velocity) time period. A random number generator is then used to decide if growth will occur. After all sites have been given a chance to grow, the heat of crystallization and the rejected second component are distributed to the nearest neighbors.

The crystal has been allowed to grow for 1/(maximum velocity) time period. The routine was written this way to limit the amount of crystal grown during a time period. Now the control is shifted to the heat transfer routine. A flow chart of the growth routine appears in Figure 8.

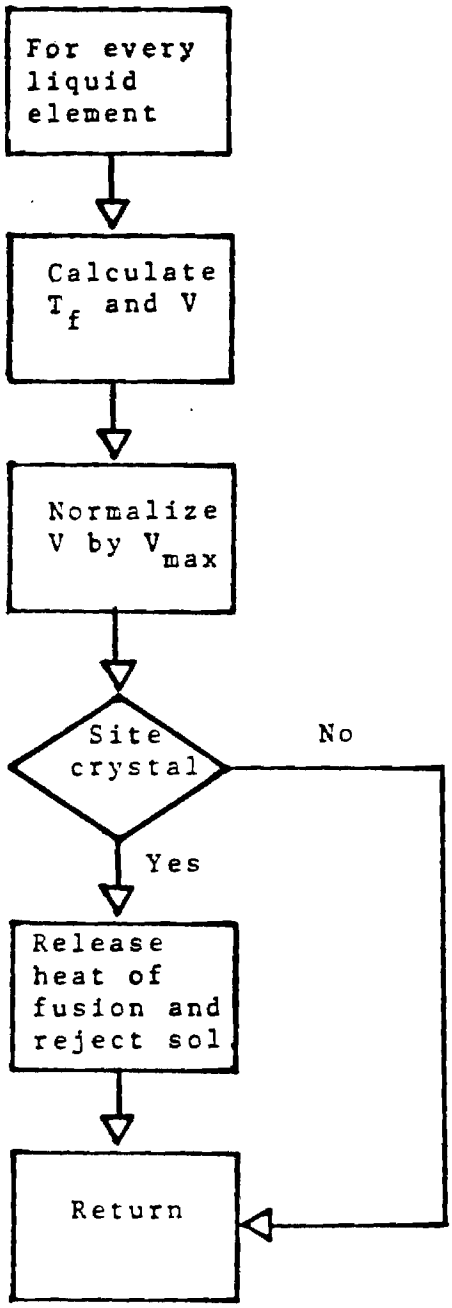

Figure 8. Flowchart for Growth Routine.

The heat transfer routine makes use of the finite difference approximations to solve the unsteady state two dimensional heat transfer equation of the form:

$$\frac{\partial T}{\partial t} = \alpha \frac{\partial^2 T}{\partial x^2} + \frac{\partial^2 T}{\partial y^2} \tag{47}$$

where α = thermal diffusivity

T = temperature

t = time

Introducing the explicit representation of Equation (47) result in:

$$\frac{T^1_{x,y} - T^0_{x,y}}{\Delta t} = \frac{\alpha}{\Delta x^2} T^0_{x+1,y} + T^0_{x-1,y} + T^0_{x,y+1} + T^0_{x,y-1} - 4T^0_{x,y}, \tag{48}$$

where $T^0_{x,y}$ = temperature at time t at location x,y

$T^1_{x,y}$ = temperature at time t+ t at location x,y

Δt = time increment

Δx = distance mesh size

A square mesh is used, so $\Delta x = \Delta y$. Assuming some value (1/n) for the modulus, $\frac{\alpha \Delta t}{\Delta x^2}$, and rearranging yields:

$$T^1_{x,y} = T^0_{x+1,y} + T^0_{x-1,y} + T^0_{x,y+1} + T^0_{x,y-1} + (n-4)\ T^0_{x,y} \tag{49}$$

Equation (49) shows that the temperature of a site at time $t+\Delta t$ can be expressed in terms of the temperature of the site and its four nearest neighbors at time t. A flow chart of the heat transfer routine appears in Figure 9.

The mass transfer routine is very similar to the heat transfer routine. The unsteady state two-dimentional diffusion equation assuming constant density and diffusivity can be written as follows:

$$\frac{\partial C_a}{\partial t} = D \frac{\partial^2 C_a}{\partial x^2} + \frac{\partial^2 C_z}{\partial y^2} \qquad (50)$$

where C_a = concentration at component a

D = mass diffusivity

the explicit form is

$$\frac{C^1_{x,y} - C^0_{x,y}}{\Delta t} = \frac{D}{\Delta x^2} \quad C^0_{x+1,y} + C^0_{x-1,y} + C^0_{x,y+1} + C^0_{x,y-1} - 4C^0_{x,y}, \qquad (51)$$

where $C^0_{x,y}$ = concentration at the t at site x,y,

$C^1_{x,y}$ = concentration at the $t+\Delta t$ at site x,y,

Figure 10 is a flow chart of the mass transfer routine. Control is then shifted to the melt routine.

The melting (dissolution) routine allows crystal sites to dissolve if the temperature and concentration conditions calculated in the previous two routines warrant it. Equilibrium freezing temperatures are calculated for each of the crystal sites next to

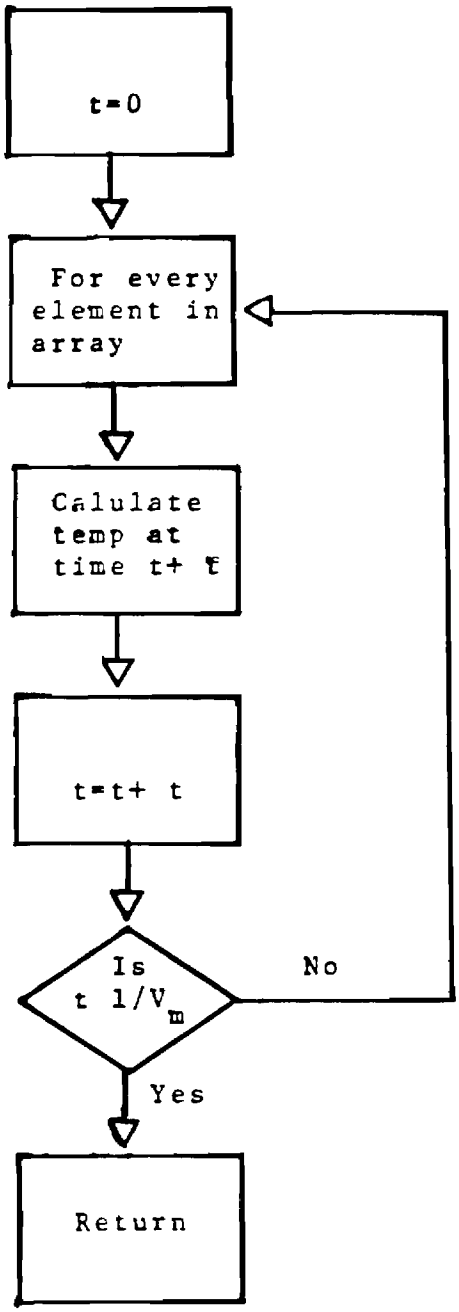

Figure 9. Flowchart of Heat Transfer Routine.

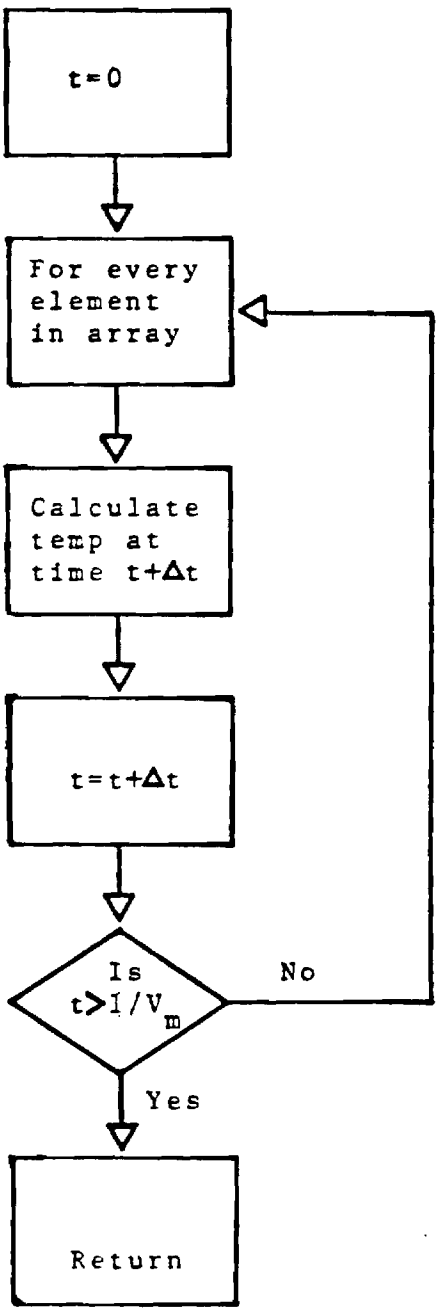

Figure 10. Flowchart of Mass Transfer Routine.

liquid neighbors and compared to the actual temperature of these sites. If the actual temperature is greater than the equilibrium freezing temperature, the sites are undersaturated. A dissolution velocity is then calculated of the same form as the one appearing in the growth routine. The dissolution velocities are then normalized. Dissolved crystal sites absorb heat from their nearest crystal neighbors. The concentration of the dissolved site and its nearest neighbors is adjusted to show the increase in concentration. A flow chart of the melt routine appears in Figure 11.

The melt routine completes the sequence for the time period defined in the growth routine so that the temperature, concentration and crystal fields all correspond to a crystal having grown for some time interval.

The process is repeated until termination conditions are met.

B. Simulation Results

The simulation was written for a binary eutectic system in Fortran V and was run on a CDC CYBER 74 computer.

The simulation was first tested to see if it followed the constitutional supporting criteria. The criteria states that the crystal would start to grow dendritically under the influence of a negative temperature gradient. In Figure 12 is an example of the results from the simulation for a negative interfacial temperature gradient. At early time it is seen that the interface is stable, but at the later time it is seen that the interface starts to grow dendritically. Stable growth was obtained under a positive interfacial temperature gradient.

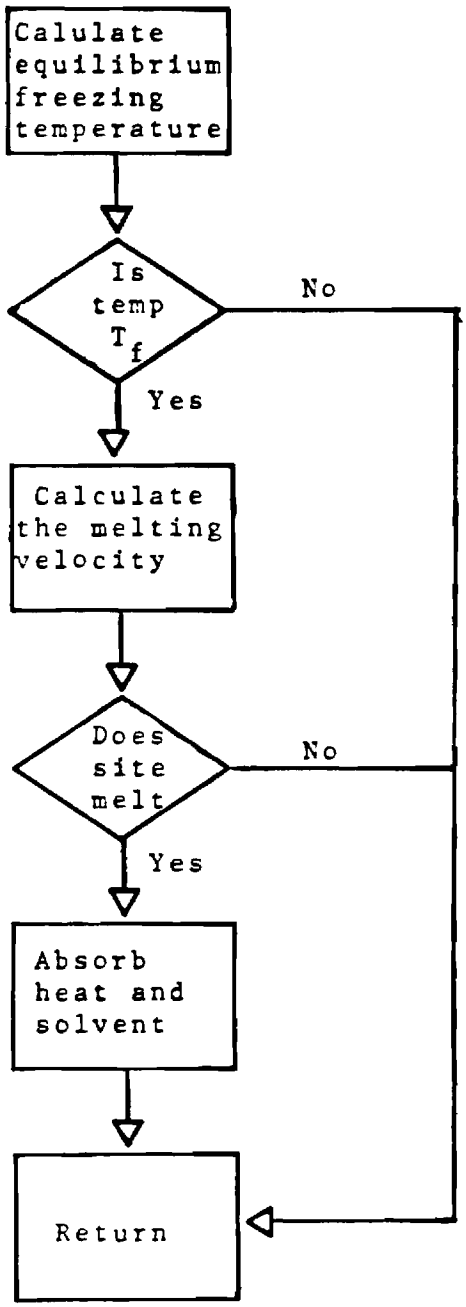

Figure 11. Flowchart of Melt Routine.

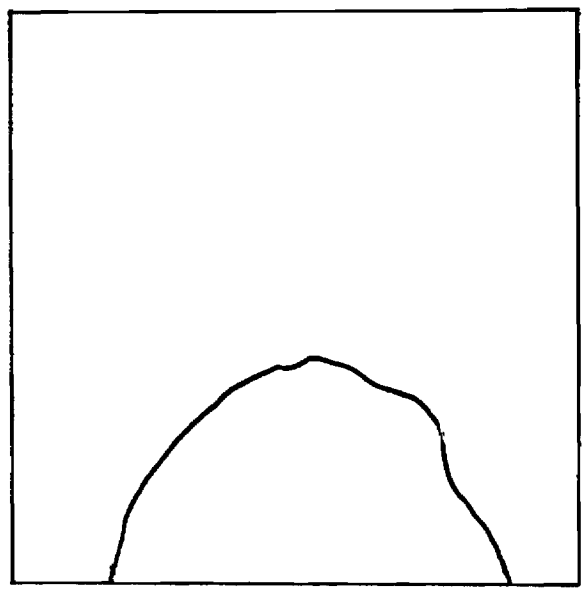

At Early Time

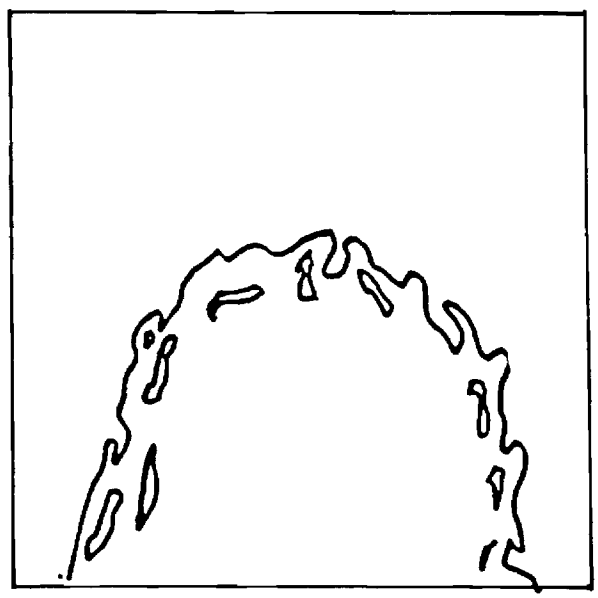

At Later Time

Figure 12. Result of Simulation with Negative Interfacial Temperature Gradient.

The simulation was applied to the water-potassium aluminum dodecahydrate system.

The simulation is a two-dimensional model, and a question arises whether one could apply this model to a three-dimensional situation. The output of the simulation can be considered a two-dimensional slice of the crystal (2). It can be shown that:

$$\frac{V_\alpha}{V} = \frac{A_\alpha}{A} \tag{52}$$

where

V_α = occlusion volume

V = total volume

A_α = occlusion area

A = total area

1. Simulated Results for the Growth of Potassium Aluminum Sulfate Dodecahydrate from Pure Aqueous Solution

In this simulation the boundary conditions imposed on the system are very important. Different temperature fields can be imposed on the system. This can be used to inspect various factors involved in crystal growth. Both velocity and interfacial temperature gradient can effect trapping and it is therefore important to vary them independently. This can be accomplished by changing the boundary conditions. The crystal growth velocity and interfacial temperature gradient can be

varied independently by imposing a temperature gradient on the system that moves with the crystal-liquid interface, The heat transfer routine automatically adjusts so that the same gradient can always be present at the leading edge of the crystal face, The growing crystal therefore always sees the same temperature and temperature gradient at the interface. The crystal growth velocity could be varied from run to run by changing the temperature at the interface,

The results of the simulation show that the critical size for occlusion formation is not a strong function of growth velocity. This can best be seen in Figure 13 which is a plot of critical size versus growth velocity. It is shown that the critical size varied from 2.0 $X10^{-3}$ m to 2.2 $X10^{-3}$ m over the range of growth velocity.

2. Simulated Results for the Growth of Potassium Aluminum Sulfate Dodecahydrate from Impure Aqueous Solution

In crystallization from impure solutions, the only type of model that could be used easily was the adsorption of the impurity on a growth site, therefore, blocking that site from crystal growth. No numerical evaluation could be made of a system that followed the adsorption model. Since no criteria for blocking active sites could be postulated. Figure 14 shows the effect of blocking active sites versus critical size for occlusion formation. It is seen that the critical size does increase due to the effect of the impurity adsorbing onto the surface.

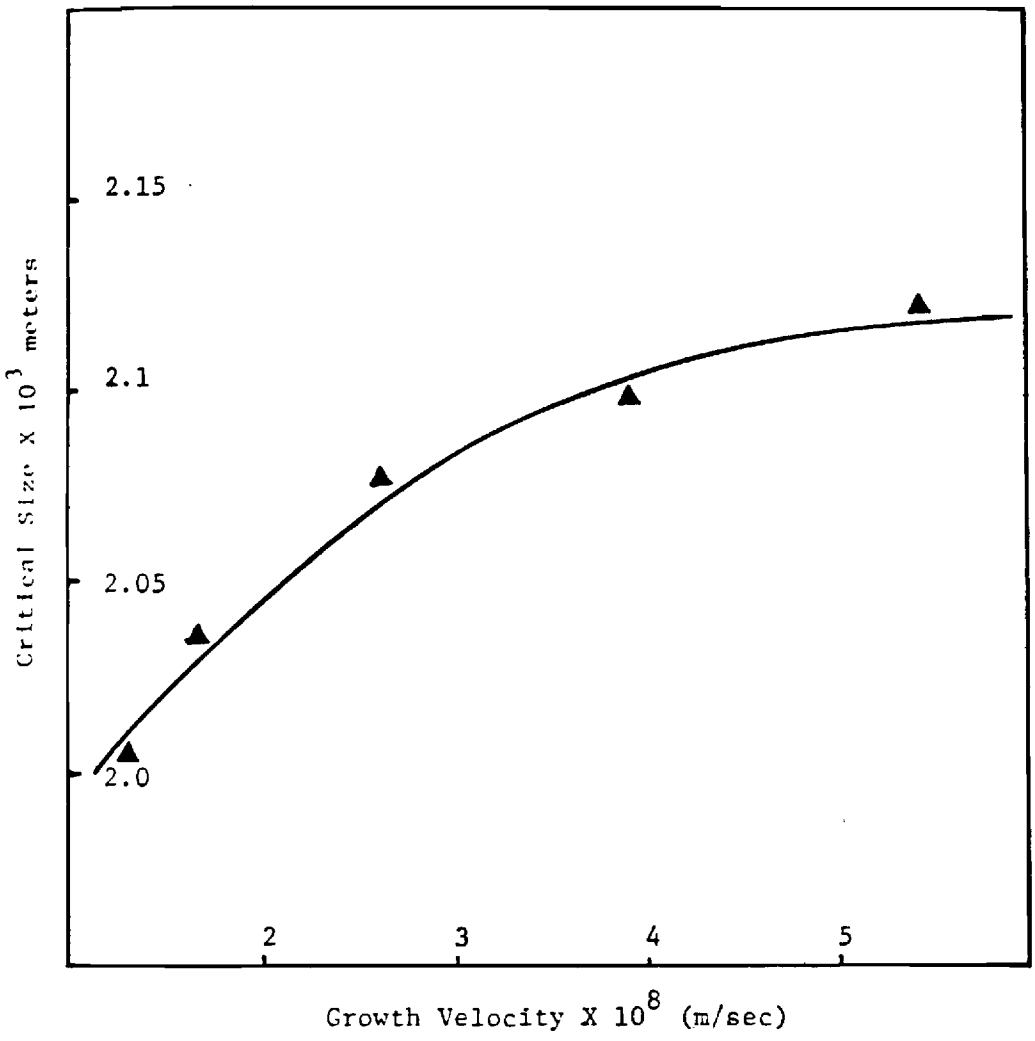

Figure 13. Critical Size vs Growth Velocity.

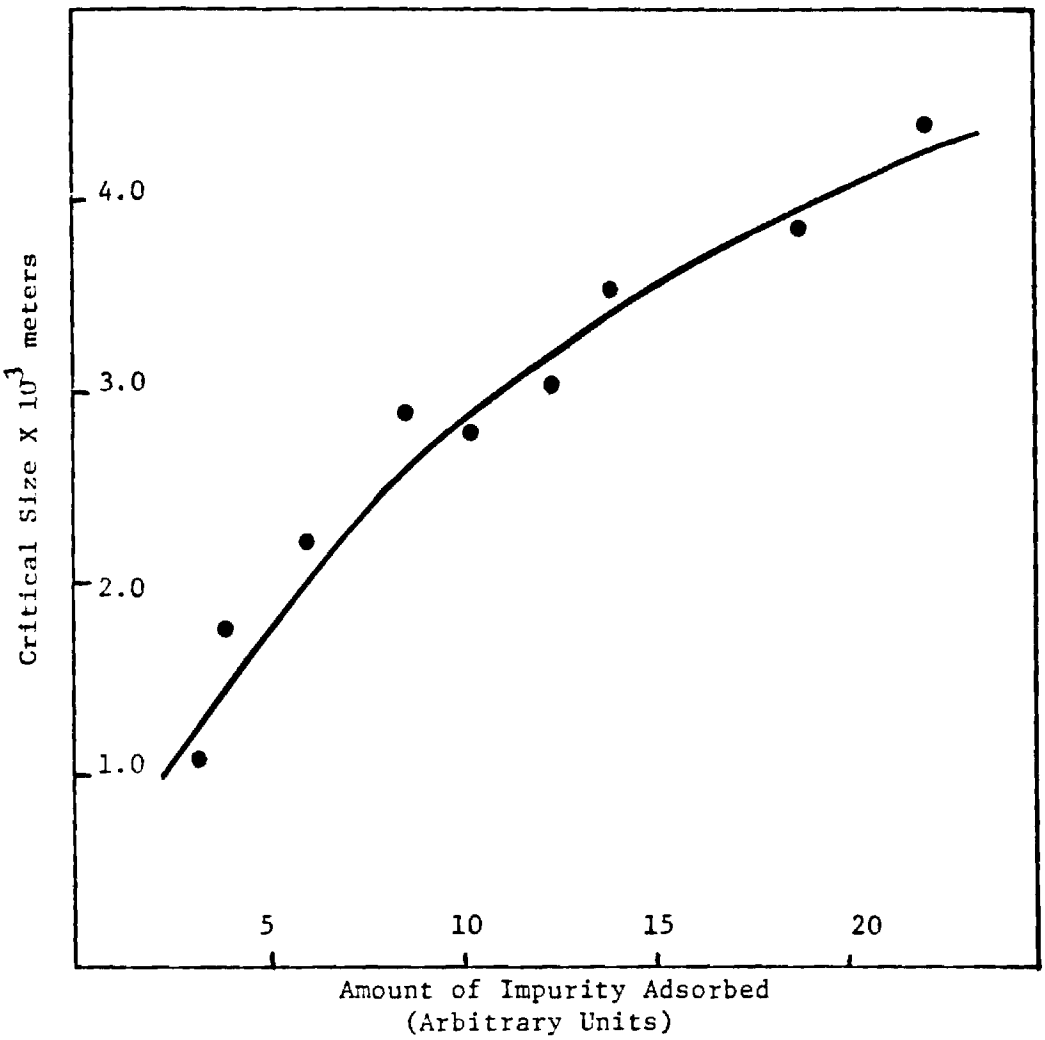

Figure 14. Critical Size vs Amount of Impurity Adsorbed.

1. Burton, W. K., Carbrera, M., and Frank, F. C., Phil. Trans. Royal Soc. London A, 243, 299 (1951).

2. Strickland-Constable, R. F. "Kinetics and Mechanisms of Crystallization," Academic Press, London, 202-205 (1968).